Metabolomic analysis to define and compare the effects of PAHs and oxygenated PAHs in developing zebrafish

Marc R. Elie[a], **Jaewoo Choi**[b], **Yasmeen M. Nkrumah-Elie**[c], **Gregory D. Gonnerman**[a], **Jan F. Stevens**[b], and **Robert L. Tanguay**[a,*]

[a] Department of Environmental and Molecular Toxicology, Environmental Health Sciences Center, Sinnhuber Aquatic Research Laboratory, Oregon State University, Corvallis, OR 97331, United States

[b] College of Pharmacy and Linus Pauling Institute, Oregon State University, Corvallis, OR 97331, United States

[c] Department of Pharmaceutical Sciences, Skaggs School of Pharmacy, University of Colorado Anschutz Medical Campus, Denver, CO 80045, United States

Abstract

Polycyclic aromatic hydrocarbons (PAHs) and their oxygenated derivatives are ubiquitously present in diesel exhaust, atmospheric particulate matter and soils sampled in urban areas. Therefore, inhalation or non-dietary ingestion of both PAHs and oxy-PAHs are major routes of exposure for people; especially young children living in these localities. While there has been extensive research on the parent PAHs, limited studies exist on the biological effects of oxy-PAHs which have been shown to be more soluble and more mobile in the environment. Additionally, investigations comparing the metabolic responses resulting from parent PAHs and oxy-PAHs exposures have not been reported. To address these current gaps, an untargeted metabolomics approach was conducted to examine the *in vivo* metabolomic profiles of developing zebrafish (*Danio rerio*) exposed to 4 μM of benz[a]anthracene (BAA) or benz[a]anthracene-7, 12-dione (BAQ). By integrating multivariate, univariate and pathway analyses, a total of 62 metabolites were significantly altered after 5 days of exposure. The marked perturbations revealed that both BAA and BAQ affect protein biosynthesis, mitochondrial function, neural development, vascular development and cardiac function. Our previous transcriptomic and genomic data were incorporated in this metabolomics study to provide a more comprehensive view of the relationship between PAH and oxy-PAH exposures on vertebrate development.

[*] Corresponding Author: Department of Environmental and Molecular Toxicology, Oregon State University, 28645 East HWY 34. Corvallis, OR 97333, USA. Fax: +1 541 737 0497. Tel.:+1 541 737 6500, robert.tanguay@oregonstate.edu (R.L. Tanguay). eliem@onid.oregonstate.edu (M. R. Elie).
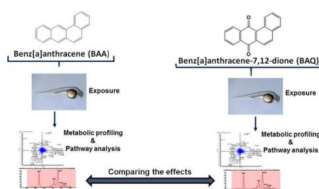
1. Introduction

Among organic pollutants, polycyclic aromatic hydrocarbons (PAHs) constitute a large and diverse class of chemicals, resulting from both natural and anthropogenic processes (Gan et al., 2009). This family of molecules is composed of two or more fused benzene rings and also includes derivatives with alkyl, nitrogen or oxygen substitutions. In recent years, environmental PAH concentrations have increased in many industrialized and developing countries, due to human activities such as fossil fuel burning and automobile exhaust (Shen et al., 2013). Increasing PAH emissions pose likely hazards to human health and may be especially acute for developing fetuses and younger children (Perera et al., 2012). Additionally, inhalation exposure to these compounds is associated with cardiac dysfunction, *in-utero* mortality, growth retardation and lower intelligence (Choi et al., 2006; Tang et al., 2008; Edwards et al., 2010; Wu et al., 2010; Jules et al., 2012). The bulk of environmental toxicity studies focus on parent-PAHs due to their potential mutagenic and carcinogenic properties; however, other studies demonstrate that oxygenated-PAH derivatives (oxy-PAHs) also negatively impact human health (Lundstedt et al., 2007). Oxy-PAHs, alongside their parent compounds, are produced during the incomplete combustion of organic matter and subsequently released into the atmosphere (Shen et al, 2011; Ringuet et al. 2012). Unlike PAHs, these derivatives are not currently monitored by international regulatory agencies; nevertheless, their physical and toxic properties warrant attention. Oxy-PAHs are more mobile in the environment than parent-PAHs because of their higher water solubility (Weigand et al., 2002). Moreover, PAHs or their oxygenated derivatives, found in diesel exhaust particles (Layshock et al., 2010; Burtscher and Schuepp, 2012), were recently suspected of being major drivers of cardiovascular, neurodegenerative and pulmonary diseases (Levesque et al., 2011; Nemmar et al., 2011; Channell, et al. 2012). Little is known about the toxicity pathways involved with these exposures during development. Consequently, there is a need for a more comprehensive understanding of the effects and the mechanisms of toxicity of PAHs and oxy-PAHs.

Environmental metabolomics is a relatively recent addition to an array of molecular techniques employed to assess the biological consequences of chemical exposures (Lankadurai et al., 2013). Changes in the metabolite patterns can be used to characterize the toxicological responses elicited from chemicals, such as PAHs or oxy-PAHs. Metabolomic analyses can be either targeted, where known metabolites are quantitated, or untargeted, during which a comprehensive analysis of all known and unknown metabolites is performed.

This latter approach allows graphical depiction of any significant differences in the patterns, which often provides information about toxicity mechanisms, pathways and possible biomarkers of exposure (Dumas et al., 2014; Prosser et al., 2014). Among the analytical instrumentations most commonly used for metabolomics studies, liquid chromatography-mass spectrometry (LC-MS) provides a powerful platform for the identification of metabolites indicative of biological and environmental perturbations (Zhou et al., 2012; Chen and Kim, 2013). Moreover, the power of the LC-MS-based metabolomics can be amplified when coupled with genomics approaches as a means to link genetic variants to phenotypic traits (Suhre and Gieger, 2012; Adamski and Suhre, 2013).

Although a vast number of organisms have been used for metabolomics studies, the zebrafish (*Danio rerio*) model has been under-utilized. As a developmental vertebrate model, the zebrafish has unique advantages for *in vivo* metabolic analyses. Much of the anatomy and physiology of fish is highly homologous to those of mammals (Eimon and Rubinstein, 2009), and zebrafish share a considerable amount of genetic identity with humans, with approximately 87% similarity (Lieschke and Currie, 2007). In addition, zebrafish embryos develop rapidly and remain transparent throughout much of organogenesis, enabling researchers to perform large-scale and high-throughput screenings at a reduced cost. (Hung et al., 2012; Santoro, 2014). Recent studies suggest that zebrafish may be an ideal reference model system for performing metabolomic-related studies (Kirkwood et al., 2012; Seth et al., 2013; Santoro, 2014). Furthermore, the metabolic changes in zebrafish are conserved in human samples (Nath et al., 2013).

Numerous embryonic zebrafish transcriptional and genetic studies have been conducted to assess the developmental toxicity of PAH and oxy-PAHs (Timme-Laragy et al., 2009; Van Tiem and Di Giulio, 2011; Goodale et al., 2013; Jayasundara et al., 2014). However, metabolic information is currently lacking. Comparing metabolic perturbations with alterations in gene transcription and protein expression, produced by PAH and oxy-PAH exposures, would be an important step toward elucidating the mechanisms of toxicity. Therefore, the overall aim of this study is to define the effects of a model PAH compound and its oxygenated derivative in zebrafish using an untargeted metabolomics approach.

2. Materials and Methods

2.1 Reagents

Benz[a]anthracene (BAA) and benz[a]anthracene-7,12-dione (BAQ) were purchased from Sigma-Aldrich (St Louis, MO, USA). Their Chemical Abstracts Service (CAS) Registry numbers, and relevant physicochemical properties are specified in Table S1. Dimethyl sulfoxide (DMSO) ACS reagent grade was obtained from J.T. Baker (Phillipsburg, NJ, USA) and methanol (high-performance liquid chromatography [HPLC] grade) was purchased from EMD Millipore (Gibbstown, NJ, USA). The purity of all chemicals exceeded 99%. Stock solutions of BAA and BAQ were made in DMSO at a concentration of 400 µM. However, for static exposures, solutions were made at a 1:100 dilution in E2 embryo medium with a 1% final DMSO concentration.

2.2 Zebrafish maintenance and embryo collection

Adult Tropical 5D strain zebrafish (*Danio rerio*) were housed at the Sinnhuber Aquatic Research Laboratory at Oregon State University. Fish care and reproductive techniques were conducted in accordance with approved Institutional Animal Care and Use Committee (IACUC) protocols. Adults fish were kept on a 14 h light/10 h dark regime in polycarbonate tanks with a recirculating water system maintained at $28° \pm 1$ °C and a pH of 7.0. Following adult spawns, fertilized embryos were collected in a clean glass Petri dish, rinsed with fish water and housed in an incubator (29 ± 1 °C) until the start of the experiment (Reimers et al., 2006).

2.3 Exposure setup

To maximize chemical exposure and uptake, the fertilized embryos were enzymatically dechorionated using a previously described method (Mandrell et al., 2012). Briefly, these embryos were developmentally staged according to Kimmel et al. (1996) and at 4 h post fertilization (hpf), they were incubated in 82 mg L^{-1} of pronase (Sigma-Aldrich; St Louis, MO, USA) at room temperature, gently agitated for 3 min and then rinsed thoroughly using an automated dechorionating system. Following rinsing, the embryos were placed in an incubator (29 ± 1 °C) for 20 min, after which greater than 95% of the chorions were removed by gentle agitation. From 6 to 120 hpf, the dechorionated embryos were batch-exposed in 20-mL amber glass vials (Ace Glass Inc., Vineland, NJ, USA).

As illustrated in Figure. S2, the static exposures were divided into three groups (vehicle control, BAA and BAQ) which were prepared in parallel. Each group consisted of 10 replicate vials of either 10 or 30 pooled embryos in 1 or 3 mL solutions, respectively. The embryos were exposed to 4 μM concentrations of BAA and BAQ or vehicle control with 1% final DMSO concentration in E2 embryo media.

2.4 Metabolite extraction

At 120 hpf, the pools of zebrafish larvae were removed from their respective exposure solutions, transferred into separate clean glass Petri dishes and rinsed with cold fish water. Subsequently, the collected larvae, from each group, were loaded in 1.5-mL safe-lock Eppendorf® tubes and chilled on ice to anesthetize and reduce enzymatic activity. After 10 min, any remaining water was removed using a microliter pipette equipped with gel-loading tips (Eppendorf; Hauppauge, NY, USA). The samples were then flash-frozen with liquid nitrogen to quench any enzymatic or metabolic activity. Immediately following the flash-freezing, 80 mg of 0.5 mm zirconium oxide beads (Next Advance, Averill Park, NY, USA) were added to each tube and the larvae were homogenized in 300 μL of extraction solvent (80:20 v/v, cold methanol/water) with a bullet blender (Next Advance, Averill Park, NY, USA). Samples were then vortexed and incubated on ice for 15 min before centrifuging for 13 min at 15,000 RCF and at 4 °C. 200 μL of supernatant, from each sample, was added into HLPC vials and stored in a freezer (−80 °C) until LC-MS/MS analysis. Figure S3 (Supplementary material) depicts the steps followed during the experimental procedure.

2.5 LC-MS/MS analysis

All samples used for metabolomic profiling were analyzed as a single batch in a random order as a means to minimize any analytical error, subjective interference and to keep the column retention shift to a minimum. To ensure the stability and repeatability of the LC-MS system, 10 μL aliquots were taken from each BAA, BAQ and vehicle control sample (in HPLC vials) and mixed to generate a pooled quality control (QC) sample, which was analyzed alongside the exposure samples.

High-pressure liquid chromatography was performed on a Shimadzu Nexera system (Shimadzu; Columbia, MD, USA) coupled to a high-resolution hybrid quadrupole-time-of-flight mass spectrometer (TripleTOF $^{®}$ 5600; AB SCIEX; Framingham, MA, USA) equipped with an electrospray ionization source. As described in a previous protocol (Kirkwood et al., 2013), chromatographic separations were carried out on an Inertsil phenyl-3 column (GL Sciences Inc., Rolling Hills Estates, CA, USA) for positive and negative ion analyses. The column size was 150×4.6 mm with a particle size of 5 μm. The flow rate was 0.4 ml/min and the injection volume was 10 μl. The mobile phases consisted of water (A) and methanol (B), both with 0.1% formic acid. The elution gradient was as follows: an initial hold at 5% B for 1 min, followed by a gradient of 5–50% B in 11 min, to 100% B at 23 min, held until 35min, then a shift to 5 % B at 37 min until 50 min. The column temperature was held at 50 °C to ensure a better repeatability between runs.

Time-of-flight (TOF) mass spectrometry (MS) was operated with an acquisition time of 0.25 s and a scan range of 70-1250 Daltons (Da). MS/MS acquisition was performed with collision energy set at 35 V and collision energy spread of 15 V. Each MS/MS scan had an accumulation time of 0.17 s and a range of 40-1250 Da using information-dependent acquisition (IDA). The source temperature was set at 500 °C and IonSpray voltage at 4.5 kV. MS and MS/MS were automatically calibrated every six injections with calibration mixtures for both ion modes.

2.6 Data processing, statistical and pathway analyses

Raw LC-MS/MS data files were first imported into MarkerView software (AB SCIEX) for initial data processing, including peak detection, peak alignment and peak integration. The following parameters were used to extract the peaks from the raw data: Retention times between 3.00 and 32.00 min.; Subtraction Offset of 10 scans; Subtraction Mult. Factor of 1.3; Noise Threshold of 50; Min. Spectral Peak Width of 15 ppm; Min. RT Peak Width of 3 scans; Retention Time Tolerance of 0.30 min.; Mass Tolerance of 10.0 ppm; 5 required samples; Maximum of 4000 peaks. Peaks with less than a 3-fold increase, compared to blank samples, were then removed from the list. Peak areas, across all samples, were subsequently normalized to the total area of the corresponding samples to balance their differences in intensities that may have arisen due to discrepancies in the sample homogenization (sample preparation). In a resultant table, the detected peaks were presented as features. A feature is defined as any identified *m/z* value detected at a unique retention time.

The normalized data were imported into IBM SPSS Statistics software version 22 (SPSS Inc., Chicago, IL, USA) for univariate analysis and into MetaboAnalyst version 3.0 (http://www.metaboanalyst.ca) for multivariate analysis (Xia et al., 2009). MarkerView was also used for multivariate analysis, specifically for principal component analysis with discriminant analysis (PCA-DA). For multivariate analyses, the data were mean-centered and Pareto-scaled to remove the offsets and adjust the importance of low and high abundance features to an equal level. Supervised multivariate modeling approaches such as Partial least-squares discriminant analysis (PLS-DA) and PCA-DA were used to determine where the greatest variation lies in the data, and also reveal the similarities or differences among the metabolite profiles of group samples relative to the different exposure groups (e.g., BAA vs. control). Additionally, cluster analysis was performed on the mean-centered and Pareto-scaled data set of the identified metabolites and was also based on the Pearson correlation coefficient. One-way ANOVA was also performed on the data set and the results were visualized by heat maps

The METLIN web-based metabolomics database (http://www.metlin.scripps.edu) was used for tentative identification of significant features. Database matching was performed in two steps, including accurate mass and MS/MS spectral matching (Smith et al., 2005). For accurate mass filtering, 5 ppm mass tolerance was used for $[M+H]^+$ or $[M-H]^-$ ions in positive and negative mode, respectively. Verification of the identified metabolites were conducted using an in-house library of standards based on the accurate mass and retention time of metabolite standards provided by IROA technologies (Bolton, MA, USA).

MetaboAnalyst was further used to assist in the analysis of the differentially expressed metabolites, identify the affected metabolic pathways and facilitate further biological interpretation. The pathway analysis module combined results from the enrichment analysis with those of the topology pathway based on database sources such as Kyoto Encyclopedia of Gene and Genomes (KEGG) and Human Metabolome Database (HMDB). For the enrichment analysis, the *p* values were generated from Fisher's exact test and represent the enrichment of certain metabolites in a particular pathway. Generally, a *p* value less than 0.05 indicates that the association between the identified metabolites and a pathway is significant and not likely due to random chance.

3. Results and Discussion

3.1 Rationale for study and experimental approach

The aim of this research was to define the metabolic alterations induced by the BAA exposure with regard to the vehicle control samples (BAA vs. control) and to directly compare these results with the perturbations produced by the BAQ exposure, in relation to the same vehicle control samples (BAQ vs. control). BAA and BAQ (Figure S1) were chosen as model compounds for a variety of reasons. Both compounds are structurally related and simultaneously detected in the atmosphere and soils of urban or polluted areas (Layshock et al., 2010; Musa Bandowe et al., 2011). Moreover, the developmental effects of BAA and BAQ were previously defined, and the results indicated that they may share the same mechanism of toxicity. It was found that both compounds elicited similar morphological responses and promoted the expression of cytochrome P4501A (CYP1A)

gene via activation of the zebrafish aryl hydrocarbon receptor 2 (AHR2) (Goodale et al. 2013; Knecht et al. 2013).

Based on the previous concentration-response studies in our laboratory 4 μM was determined to be the optimum concentration for both compounds to elicit sub-lethal metabolic responses in zebrafish. Additionally, no significant teratogenic effects were observed at the 4 μM doses for BAA and BAQ treatments relative to the vehicle control (Fig S4). Two sets of experiments were preliminarily conducted with 3 replicate vials (n = 3) for each group (BAA, BAQ and vehicle control). The first set consisted of replicates of 10-pooled embryos for each group, while the second set was comprised of replicates of 30-pooled embryos. No significant mortalities were observed during the exposure period and the metabolite extractions were subsequently performed with 80:20 (v/v) cold methanol and water (Kirkwood et al. 2013). It was determined that 30-embryos samples yielded more metabolic features with sufficient intensities compared to the 10-embryos samples. Subsequently, a statistical power analysis was conducted with the preliminary 30 embryo pools to determine the minimum sample size or minimum number of replicates in this case. As shown in Figure S5, a 74% and 80% power to detect BAA- and BAQ-induced metabolic differences (compared to the control) were obtained with 10 replicates per group (n = 10/group). Hereafter, a sample size of 10 replicates of 30 embryo pools was selected for the study.

3.2 Validity of instrumental analysis

As described in the *Materials and methods* section, the experimental approach of this study consisted of sample collection, extraction and LC-MS/MS analysis. However, prior to analyzing the untargeted metabolite profile of the hydrophilic extracts, a validation of the analytical method was completed. Analytical variance arises from the spread of measured values (e.g., sample preparation retention times, peak intensities) observed from multiple measurements of the same biological sample (Moseley, 2013), and such a variance can skew successive technical steps such as data processing. The reproducibility and stability of the LC-MS/MS method were evaluated by examining the distribution of the relative standard deviations (%RSD) of the peak areas (of all the detected features) from the pooled QC sample that was repetitively analyzed after every five injections throughout the analytical run. The results revealed that for all six QC injections, 82.4% and 76.0% of the differential features had a %RSD of less than 20% in the positive and negative ion mode, respectively (Figure S6). Additionally, the positive and negative ion mode PCA scores plots showed that all of the repeated QC samples were closely clustered demonstrating the robustness of our analytical method (Figure S7). Thus, the analyses under the defined conditions were stable and acceptable to further explore the information derived from the *in vivo* exposures.

3.3 Metabolic profiling using multivariate pattern recognition analysis

The features detected in at least 50% of the samples, in any of the three groups (vehicle control, BAA and BAQ), were selected for differential metabolite analysis. To directly evaluate the induced metabolic alterations and help establish whether or not differences in metabolic profiles exist among the groups, pattern recognition techniques such as PLS-DA and PCA-DA were both applied to the data set. The results are represented as scores plots, in

which a group of samples that displayed a particular metabolic profile (e.g., control samples), clustered together in a particular area of the plot.

As shown in Figures 1 and 2, the two-dimensional score plots of the PLS-DA and PCA-DA models both demonstrated that the BAA and BAQ groups were separated from each other and from the control group in the PC1 direction. The clear separation from the vehicle control group indicate that the metabolic perturbations were associated with BAA and BAQ exposures. In the positive ion mode, PC1 and PC2 components of the PLS-DA scores plot explained 51.3 % of the total variance; while D1 and D2 components of the PCA-DA plot explained 99.5% of the total variance (Fig.1). In the negative ion mode data set, PC1 and PC2 components of the PLS-DA scores plot explain 48 % of the total variance, and D1 and D2 of the PCA-DA plot explained 100% of the total variance (Fig. 2). These results indicate that the LC-MS based method in combination with multivariate pattern recognition, generated a tangible representation of the metabolic changes associated with BAA and BAQ developmental exposures.

3.4 Univariate statistical comparison between the treated groups and the control group

The untargeted metabolomics approach of this study was aimed at the discovery of those metabolites that are varied between two independent groups (e.g., BAA vs control or BAQ vs control). The fit of our group samples to the assumptions for parametric or non-parametric tests was examined with the Shapiro-Wilk test for normality (Razali and Wah, 2011) and the Levene's test for equality of variances (Gastwirth et al., 2009). Table S2 shows the percentage of features that met normality and homogeneity assumptions in our data set. On average, 70% of detected features met both normality and equality of variance assumptions. Based on these results, the Welch *t*-test was used to evaluate significance due to its robustness when dealing with deviations of normal distributions and moderate unequal variances in the data set (Skovlund and Fenstad, 2001; Fagerland and Sandvik, 2009; Ruxton, 2006).

Using this approach, the BAA and BAQ groups were compared to the vehicle control group to find the most significantly altered metabolites between them. In addition, to reduce false discoveries and to improve the statistical robustness in finding differential metabolites, the false discovery rate (FDR) correction was performed using the Benjamin and Hochberg method (Benjamin and Hochberg, 1995). Metabolite features were considered statistically significant with *p* values less than 0.05 and FDR results below 0.05. Out of a total of 147 identified features, 63 metabolites were found to fulfill the statistical significance criteria for the BAA-control and BAQ-control comparisons in both positive and negative ion modes. The significant metabolites were identified based on accurate mass, spectral matching with the METLIN metabolite database (Zhu et al., 2013), and were further confirmed based on comparisons with known standards and their retention times. Identified metabolites, the fold changes with *p* and FDR values are presented in Table S3. These significantly different metabolites were amino acids, amino ketones, polyamines, nucleosides, organic acids, fatty acids, carbohydrates and sugar phosphates. Furthermore, it should be noted that more than 80% of the identified metabolites (Table S3) had *p* and FDR values less than 0.01, which is

considerably less than the cut-off value of 0.05 and indicating that the observed alterations are statistically robust.

3.5 Pathway Analysis

Following the identification of the significant differential metabolites (Table S3), a targeted data analysis approach was employed. Pathway enrichment analysis combined with the topology analysis was conducted using Metaboanalyst (Xia et al., 2012) to reveal the most relevant pathways influenced by the respective BAA and BAQ exposures (Figure 3). Based on the KEGG pathway database and previous pathway research on the zebrafish metabolome, it was discovered that both BAA and BAQ exposures are responsible for the perturbation of: 1) glutathione metabolism; 2) glycine, serine and threonine metabolism; 3) cysteine and methionine metabolism; 4) purne metabolism; 5) phenylalanine metabolism; 6) phenylalanine, tyrosine and tryptophan metabolism; 7) aminoacyl-tRNA biosynthesis.

3.5.1. Glutathione metabolism—Glutathione (GSH) biosynthesis and metabolism encompass other metabolic pathways such as glycine, serine, threonine metabolism and the cysteine and methionine metabolism (Noctor et al., 1998; Lu, 2013); which have all been shown to be influenced by the BAA and BAQ exposures. A significant increase in GSH ($p <$ 0.05) was associated with BAA and BAQ exposures relative to the vehicle control group. GSH is considered as an efficient antioxidant, defending against oxidative stress in cells through its ability to scavenge and reduce reactive oxygen species (ROS) (Haenen and Bast, 2014). Moreover, serine, threonine, cystathione, S-adenosylmethionine and S-adenosylhomocysteine were found at increased levels for both exposures. These amino acids and amino acid derivatives are all necessary for the formation of GSH (Figure S8). In addition, methionine levels were increased by a 2.3- and a 1.8-fold change from the BAA and BAQ exposures, respectively. This sulfur containing amino acid also plays a critical role in the biosynthesis of GSH and has been shown to be a chemopreventive agent due to its ability to interfere with the oxidative DNA damage induced by benzo[a]pyrene (B[a]P), a known carcinogenic PAH compound (Roh et al., 2012).

In our previous studies (Goodale et al., 2013; Knecht et al., 2013; Goodale et al. 2015), BAA and BAQ developmental toxicities were examined by investigating the global differences in transcription with whole genome mRNA sequencing and quantifying the expression of a battery of known redox-affected genes. These studies revealed that many of the transcripts elevated by BAA were similarly increased by BAQ, and in concordance with the metabolomics reported here, oxidative stress was a component of the responses of BAA- and BAQ-exposed embryos (Goodale et al., 2013; Goodale et al., 2015). Additionally, several genes important in cellular detoxification and protection from oxidative stress, such as glutathione S-transferase (GST), glutathione peroxidase (GPx), were significantly elevated (p < 0.05) in embryos exposed to BAQ for 48 hpf (Knecht et al., 2013). BAQ exposure also elicited the induction of the catalytic subunit of glutamate-cysteine ligase (GCLC), which catalyzes the rate-limiting step of GSH synthesis (Hayes and Pulford, 1995). This is consistent with the hypothesis that BAA and BAQ-induced the production of GSH as an adaptive stress response.

3.5.2. Purine metabolism—As shown in Figure 3, purine metabolism was the most affected pathway ($p < 0.00001$) for both BAA and BAQ exposures. Purine metabolism, also called purine nucleotide catabolism (PNC), may be a component of the homeostatic response of mitochondria to oxidative stress. Studies have shown that PAHs accumulate in the mitochondria, due to its high lipid content, and subsequently induce mitochondrial oxidative damage and reduce ATP levels (Xia et al., 2004; Farris et al., 2005; Meyer et al., 2013). It has been hypothesized that, in response to decreased energy charge or oxidative damage, there is a mitochondrial homeostatic response to activate and increase purine catabolism to produce cellular antioxidant uric acid (Kristal et al., 1999) and to salvage free purine bases to restore nucleotide levels, including ATP (Ong et al., 2010; Liechti and Goldberg, 2012). The metabolomics analyses reveal a significant increase ($p < 0.05$) in the production of uric acid and other catabolites (e.g., guanosine, hypoxanthine, inosine and xanthine), following BAA and BAQ exposures (Figure S9). Additionally, upregulation of inosine monophosphate and guanosine monophosphate nucleotides were observed, thus, supporting the hypothesis that purine bases are salvaged and reutilized during times of oxidative stress.

Moreover, the effect of BAQ on mitochondrial function was evaluated by measuring mitochondrial respiration and hydrogen production (Knecht et al., 2013). Correlating with our present metabolomics findings, the previous results showed that BAQ-exposed embryos had significantly decreased ATP-linked oxygen consumption rates and an apparent trend toward lower mitochondrial oxygen capacity compared to the vehicle controls, all of which implies a mitochondrial response to oxidative stress (Dranka et al., 2011). Furthermore, PAH exposures and induced mitochondrial oxidative damage are associated with cardiac ischemia and hypoxia (Burstyn et al., 2005; Li et al., 2015). In our previous gene-expression study, BAQ exposure was associated with altered transcription of several hypoxia-related signaling genes (Goodale et al., 2015). Additionally, genes involved in vasculature development and low-blood flow signaling were misexpressed in BAA-exposed embryos (Goodale et al., 2013). It is also noteworthy that inosine, a candidate biomarker for cardiac ischemia (Farthing et al., 2006; Becker et al., 2011), had the highest fold change out of all of the identified metabolites following BAA exposure (Table S3). Collectively, the present metabolome and previous results suggest that vascular development and possibly cardiac dysfunction are associated with BAA and BAQ exposures.

3.5.3. Phenylalanine, tyrosine and tryptophan biosynthesis—Phenylalanine (Phe), tyrosine (Tyr) and tryptophan (Tryp) metabolites were significantly increased ($p < 0.05$) when comparing each exposure group (BAA and BAQ) to the vehicle control group (Fig. S10). Both Phe and Tyr are precursors of the catecholamine neurotransmitters, dopamine, norepinephrine, and epinephrine, while Tryp is the precursor of serotonin, which is a brain neurotransmitter. Dopamine (DA) synthesis was significantly ($p < 0.05$) induced after both BAA and BAQ exposures (Table S3). Increases in serotonin (5HT) levels were also observed following BAA (2.0-fold) and BAQ (1.7-fold) exposure, relative to vehicle control group. As a brain neurotransmitter, 5HT modulates several behavioral and neuropsychological processes such as sleep, aggression, appetite, memory and rhythmic motor patterns (Berger et al., 2009).

The significant alterations in DA and 5HT and the neurotransmitter-precursor metabolites (Tyr, Phe, Tryp) may be predictive of developmental neurobehavioral effects associated with BAA and BAQ. PAH exposures in rats and in humans have been associated with neurobehavioral effects (Edwards et al., 2010; Xia et al., 2011; Perera et al., 2012); however limited data exist on the behavioral effects of oxy-PAHs. The present findings show that both BAA and BAQ exposures perturb levels of DA and 5HT neurotransmitters and their respective precursors, implying that both of these compounds may have a similar mechanism and involvement in the dysfunction of a number neurological and behavioral processes. Gesto et al. (2006; 2008; 2009) demonstrated that PAH and oxy-PAH exposures altered the levels of DA and 5HT metabolites in the brain of rainbow trout. Moreover, other reports have associated zebrafish central nervous system (CNS) effects with exposure to various PAHs (Vignet et al. 2014a; 2014b). In their studies, adult zebrafish which were developmentally exposed to individual PAHs or PAH mixtures, exhibited impaired locomotor activity, and increased anxiety compared to non-exposed fish. Additionally, similar results were reported using Japanese medaka embryos exposed to BAA (Le Bihanic et al., 2015), suggesting that PAHs are developmental neurotoxicants. The probability that some oxy-PAHs are also developmental neurotoxicants is high, however, a more comprehensive analysis is still needed.

3.5.4. Aminoacyl-tRNA biosynthesis

The aminoacyl-tRNA (aa-tRNA) biosynthesis was also significantly affected by both BAA and BAQ exposures (Figure 3). The aa-tRNA pathway and aminoacyl tRNA synthetase (aaRS) enzymes are key factors required for protein biosynthesis (Ibba and Söll, 2000). Exposure to BAA and BAQ caused a significant increase ($p < 0.05$) in levels of all identified cellular amino acids (Table S2). This is indicative of decreased protein syntheses. Hradec (1967) reported that carcinogenic PAHs, such as B[a]P, alter the activity of various aaRS enzymes, in addition to the inhibition of the sequential steps involved protein synthesis. However, the exact mechanism by which PAHs alter the aa-tRNA pathway was not identified. Shen and Yu (2008) and Kalkhof et al. (2014) found that a similar decreased in protein synthesis was associated with exposure to with B[a]P and a B[a]P metabolite. Their results showed that most subunits of eukaryotic translation initiation factors (EIFs) and involved proteins were down-regulated after 24 h of exposures. Hence, the decreased metabolic activity associated with PAHs and the enhanced levels of amino acids observed suggest that translation was suppressed following developmental exposure to BAA and BAQ.

3.6. Comparing the metabolic profiles of the exposure groups

As described above, exposure to BAA and BAQ resulted in similar metabolite profiles. However, it is noted that developmental BAQ exposure led to an overall lower magnitude fold changes compared to BAA exposure (Table S3). The significantly altered and identified metabolites were subjected to hierarchical clustering to determine variations between exposures relative to the control group. For both positive and negative ion modes, the generated heat maps (Figs. 4 and S11) revealed variations between replicate samples within each group, which could be due to biological variation. Although there were overlaps in the metabolic profiles between the two exposures, the fold-change of metabolite levels were different. As shown in Figure 4, there is a slight increase in metabolites when comparing

changes between the control and BAQ group (from right to left in Figure 4); however, a more substantial increase in metabolic alterations can be observed when comparing the vehicle control to the BAA group. Inherent biological variations could partially explain the response pattern, the different physical properties of these compounds likely plays an important role; specifically bioavailability may underlie the difference observed in metabolic perturbations. Future body-burden studies are needed to define BAA- and BAQ-bioavailability under these experimental conditions.

4. Conclusions

To address current knowledge gaps, a study was conducted to define and compare the effects of a model PAH compound and its oxygenated derivative on the developing zebrafish metabolome. By incorporating *in vivo* metabolic profiling with multivariate pattern recognition and pathway analysis, the metabolomics data revealed that BAA and BAQ exposures were strongly associated with changes known to affect protein biosynthesis, mitochondrial dysfunction (oxidative stress), neural development, disturbance in vascular development and cardiac development function (cardiac toxicity). These findings generally concur with previous transcriptomics studies associated with the toxicological responses and effects of other PAHs and oxygenated PAHs (Goodale et al., 2013; Gurbani et al., 2013; Jayasundara et al., 2014). Our results demonstrated the utility of LC-MS-based metabolomics combined with the developmental zebrafish model to provide deeper mechanistic insights into the connections between chemical exposure and profound effects on organisms. Application of this approach to more structurally diverse PAHs and oxy-PAHs could greatly expand the utility of metabolomics for predicting the structure-activity relationships and hazard potential of a very diverse and ubiquitous class of contaminants.

Supplementary Material

Refer to Web version on PubMed Central for supplementary material.

Acknowledgements

References

Adamski J, Suhre K. Metabolomics platforms for genome wide association studies—linking the genome to the metabolome. Curr. Opin. Biotechnol. 2013; 24:39–47. [PubMed: 23102864]

Becker BF, Fischer J, Hartmann H, Chen CC, Sommerhoff CP, Tschoep J, Annecke T. Inosine, not adenosine, initiates endothelial glycocalyx degradation in cardiac ischemia and hypoxia. Nucleos. Nucleot. Nucl. 2011; 30:1161–1167.

Benjamini Y, Hochberg Y. Controlling the false discovery rate-a practical and powerful approach to multiple testing. J. Roy. Stat. Soc. B Methodol. 1995; 57:289–300.

Berger M, Gray JA, Roth BL. The expanded biology of serotonin. Annu. Rev. Med. 2009; 60:355–366. [PubMed: 19630576]

Burstyn I, Kromhout H, Partanen T, Svane O, Langård S, Ahrens W, Boffetta P. Polycyclic aromatic hydrocarbons and fatal ischemic heart disease. Epidemiology. 2005; 16:744–750. [PubMed: 16222163]

Burtscher H, Schüepp K. The occurrence of ultrafine particles in the specific environment of children. Paediatr. Respir. Rev. 2012; 13:89–94. [PubMed: 22475254]

Channell MM, Paffett ML, Devlin RB, Madden MC, Campen MJ. Circulating factors induce coronary endothelial cell activation following exposure to inhaled diesel exhaust and nitrogen dioxide in humans: evidence from a novel translational in vitro model. Toxicol. Sci. 2012; 127:179–186. [PubMed: 22331494]

Chen C, Kim S. LC-MS-based Metabolomics of Xenobiotic-induced Toxicities. Comput. Struct. Biotechnol. J. 2013; 4:e201301008. [PubMed: 24688689]

Choi H, Jedrychowski W, Spengler J, Camann DE, Whyatt RM, Rauh V, Tsai WY, Perera FP. International studies of prenatal exposure to polycyclic aromatic hydrocarbons and fetal growth. Environ. Health Perspect. 2006; 114:1744–1750. [PubMed: 17107862]

Dranka BP, Benavides GA, Diers AR, Giordano S, Zelickson BR, Reily C, Darley-Usmar VM. Assessing bioenergetic function in response to oxidative stress by metabolic profiling. Free Radic. Biol. Med. 2011; 51:1621–1635. [PubMed: 21872656]

Dumas ME, Kinross J, Nicholson JK. Metabolic phenotyping and systems biology approaches to understanding metabolic syndrome and fatty liver disease. Gastroenterology. 2014; 146:46–62. [PubMed: 24211299]

Edwards SC, Jedrychowski W, Butscher M, Camann D, Kieltyka A, Mroz E, Flak E, Li Z, Wang S, Rauh V, Perera F. Prenatal exposure to airborne polycyclic aromatic hydrocarbons and children's intelligence at 5 years of age in a prospective cohort study in Poland. Environ. Health Perspect. 2010; 118:1326–1331. [PubMed: 20406721]

Eimon PM, Rubinstein AL. The use of in vivo zebrafish assays in drug toxicity screening. Expert. Opin. Drug Metab. Toxicol. 2009; 5:393–401. [PubMed: 19368493]

Fagerland MW, Sandvik L. Performance of five two-sample location tests for skewed distributions with unequal variances. Contemp. Clin. Trials. 2009; 30:490–496. [PubMed: 19577012]

Fariss MW, Chan CB, Patel M, Van Houten B, Orrenius S. Role of mitochondria in toxic oxidative stress. Mol. Interv. 2005; 5:94–111. [PubMed: 15821158]

Farthing D, Xi L, Gehr L, Sica D, Larus T, Karnes HT. High-performance liquid chromatography (HPLC) determination of inosine, a potential biomarker for initial cardiac ischaemia, using isolated mouse hearts. Biomarkers. 2006; 11:449–459. [PubMed: 16966161]

Gan S, Lau EV, Ng HK. Remediation of soils contaminated with polycyclic aromatic hydrocarbons (PAHs). J. Hazard. Mater. 2009; 172:532–549. [PubMed: 19700241]

Gastwirth JL, Gel YR, Miao W. The impact of Levene's test of equality of variances on statistical theory and practice. Statist. Sci. 2009; 24:343–360.

Gesto M, Tintos A, Soengas JL, Miguez JM. Effects of acute and prolonged naphthalene exposure on brain monoaminergic neurotransmitters in rainbow trout (Oncorhynchusmykiss). Comp. Biochem. Physiol. C. 2006; 144:173–183.

Gesto M, Soengas JL, Miguez JM. Acute and prolonged stress responses of brain monoaminergic activity and plasma cortisol levels in rainbow trout are modified by PAHs (naphthalene, betanaphthoflavone and benzo(a)pyrene treatment. Aquat. Toxicol. 2008; 86:341–351. [PubMed: 18180048]

Gesto M, Tintos A, Soengas JL, Miguez JM. Beta-Naphthoflavone and benzo(a)pyrene alter dopaminergic, noradrenergic, and serotonergic systems in brain and pituitary of rainbow trout (Oncorhynchus mykiss). Ecotoxicol. Environ. Saf. 2009; 72:191–198. [PubMed: 18462795]

Goodale BC, Tilton SC, Corvi MM, Wilson GR, Janszen DB, Anderson KA, Tanguay RL. Structurally distinct polycyclic aromatic hydrocarbons induce differential transcriptional responses in developing zebrafish. Toxicol. Appl. Pharmacol. 2013; 272:656–670. [PubMed: 23656968]

Goodale BC, La Du J, Tilton SC, Sullivan CM, Waters KM, Tanguay RL. Oxygenated PAHs, benzanthrone and benz[a]anthracene-7,12-dione disrupt expression of distinct sets of genes

regulated by aryl hydrocarbon receptor during development. Toxicological Sciences. 2015 Submitted to.

Gurbani D, Bharti SK, Kumar A, Pandey AK, Ana GR, Verma A, Dhawan A. Polycyclic aromatic hydrocarbons and their quinones modulate the metabolic profile and induce DNA damage in human alveolar and bronchiolar cells. Int. J. Hyg. Environ. Health. 2013; 216:553–565. [PubMed: 23735462]

Haenen GR, Bast A. Glutathione revisited: a better scavenger than previously thought. Front. Pharmacol. 2014; 5:260. [PubMed: 25505886]

Hayes JD, Pulford DJ. The glutathione S-transferase supergene family: regulation of GST and the contribution of the isoenzymes to cancer chemoprotection and drug resistance. Crit. Rev. Biochem. Mol. Biol. 1995; 30:445–600. [PubMed: 8770536]

Hradec J. Effect of some polycyclic aromatic hydrocarbons on protein synthesis *in vitro*. Biochem. J. 1967; 105:251–259. [PubMed: 4168142]

Huang SM, Xu F, Lam SH, Gong Z, Ong CN. Metabolomics of developing zebrafish embryos using gas chromatography-and liquid chromatography-mass spectrometry. Mol. BioSyst. 2013; 9:1372–1380. [PubMed: 23475132]

Hung MW, Zhang ZJ, Li S, Lei B, Yuan S, Cui GZ, Lee SMY. From omics to drug metabolism and high content screen of natural product in zebrafish: a new model for discovery of neuroactive compound. Evid. Based Complement. Alternat. Med. 2012; 2012:605303. [PubMed: 22919414]

Ibba M, Söll D. Aminoacyl-tRNA synthesis. Annu. Rev. Biochem. 2000; 69:617–650. [PubMed: 10966471]

Jayasundara N, Garner LVT, Meyer JN, Erwin KN, Di Giulio RT. AHR2-mediated transcriptomic responses underlying the synergistic cardiac developmental toxicity of PAHs. Toxicol. Sci. 2014; 143:469–481. [PubMed: 25412620]

Jules GE, Pratap S, Ramesh A, Hood DB. In utero exposure to benzo(a)pyrene predisposes offspring to cardiovascular dysfunction in later-life. Toxicology. 2012; 295:56–67. [PubMed: 22374506]

Kalkhof S, Dautel F, Loguercio S, Baumann S, Trump S, Jungnickel H, von Bergen M. Pathway and time-resolved benzo[a]pyrene toxicity on hepa1c1c7 cells at toxic and subtoxic exposure. J. Proteome Res. 2014; 14:164–182. [PubMed: 25362887]

Kimmel CB, Ballard WW, Kimmel SR, Ullmann B, Schilling TF. Stages of embryonic development of the zebrafish. Dev. Dyn. 1995; 203:253–310. [PubMed: 8589427]

Kirkwood JS, Lebold KM, Miranda CL, Wright CL, Miller GW, Tanguay RL, Stevens JF. Vitamin C deficiency activates the purine nucleotide cycle in zebrafish. J. Biol. Chem. 2012; 287:3833–3841. [PubMed: 22170049]

Kirkwood JS, Maier C, Stevens JF. Simultaneous, Untargeted Metabolic Profiling of Polar and Nonpolar Metabolites by LC-Q-TOF Mass Spectrometry. Curr. Protoc. Toxicol. 2013; 4:4–39.

Knecht AL, Goodale BC, Truong L, Simonich MT, Swanson AJ, Matzke MM, Tanguay RL. Comparative developmental toxicity of environmentally relevant oxygenated PAHs. Toxicol. Appl. Pharmacol. 2013; 271:266–275. [PubMed: 23684558]

Kristal BS, Vigneau-Callahan KE, Moskowitz AJ, Matson WR. Purine catabolism: links to mitochondrial respiration and antioxidant defenses? Arch. Biochem. Biophys. 1999; 370:22–33. [PubMed: 10496973]

Lankadurai BP, Nagato EG, Simpson MJ. Environmental metabolomics: an emerging approach to study organism responses to environmental stressors. Environ. Rev. 2013; 21:180–205.

Layshock JA, Wilson G, Anderson KA. Ketone and quinone-substituted polycyclic aromatic hydrocarbons in mussel tissue, sediment, urban dust, and diesel particulate matrices. Environ. Toxicol. Chem. 2010; 29:2450–2460. [PubMed: 20830751]

Li R, Kou X, Geng H, Xie J, Tian J, Cai Z, Dong C. Mitochondrial damage: An important mechanism of ambient $PM_{2.5}$ exposure-induced acute heart injury in rats. J. Hazard. Mater. 2015; 287:392–401. [PubMed: 25677476]

Liechti G, Goldberg JB. *Helicobacter pylori* relies primarily on the purine salvage pathway for purine nucleotide biosynthesis. J. Bacteriol. 2012; 194:839–854. [PubMed: 22194455]

Lieschke GJ, Currie PD. Animal models of human disease: zebrafish swim into view. Nat. Rev. Genet. 2007; 8:353–367. [PubMed: 17440532]

Le Bihanic F, Sommard V, Pichon A, Grasset J, Berrada S, Budzinski H, Cachot J. Environmental concentrations of benz[a]anthracene induce developmental defects and DNA damage and impair photomotor response in Japanese medaka larvae. Ecotoxicol. Environ. Saf. 2015; 113:321–328. [PubMed: 25528488]

Levesque S, Surace MJ, McDonald J, Block ML. Air pollution and the brain: subchronic diesel exhaust exposure causes neuroinflammation and elevates early markers of neurodegenerative disease. J. Neuroinflammation. 2011; 8:105. [PubMed: 21864400]

Lu SC. Glutathione synthesis. Biochim. Biophys. Acta. 2013; 5:3143–3153. [PubMed: 22995213]

Lundstedt S, White PA, Lemieux CL, Lynes KD, Lambert IB, Oberg L, Haglund P, Tysklind M. Sources, fate, and toxic hazards of oxygenated polycyclic aromatic hydrocarbons (PAHs) at PAH contaminated sites. Ambio. 2007; 36:475–485. [PubMed: 17985702]

Mandrell D, Truong L, Jephson C, Sarker MR, Moore A, Lang C, Simonich MT, Tanguay RL. Automated zebrafish chorion removal and single embryo placement. J. Lab. Autom. 2012; 17:66–74. [PubMed: 22357610]

Meyer JN, Leung MC, Rooney JP, Sendoel A, Hengartner MO, Kisby GE, Bess AS. Mitochondria as a target of environmental toxicants. Toxicol. Sci. 2013; 134:1–17. [PubMed: 23629515]

Moseley HN. Error Analysis and Propagation in Metabolomics Data Analysis. Comput. Struct. Biotechnol. J. 2013; 4:e201301006. [PubMed: 23667718]

Musa Bandowe BA, Sobocka J, Wilcke W. Oxygen-containing polycyclic aromatic hydrocarbons (OPAHs) in urban soils of Bratislava, Slovakia: Patterns, relation to PAHs and vertical distribution. Environ. Pollut. 2011; 159:539–549. [PubMed: 21095050]

Nath AK, Roberts LD, Liu Y, Mahon SB, Kim S, Ryu JH, Peterson RT. Chemical and metabolomic screens identify novel biomarkers and antidotes for cyanide exposure. FASEB J. 2013; 27:1928–1938. [PubMed: 23345455]

Nemmar A, Al-Salam S, Zia S, Marzouqi F, Al-Dhaheri A, Subramaniyan D, Dhanasekaran S, Yasin J, Ali BH, Kazzam EE. Contrasting actions of diesel exhaust particles on the pulmonary and cardiovascular systems and the effects of thymoquinone. Br. J. Pharmacol. 2011; 164:1871–1882. [PubMed: 21501145]

Noctor G, Arisi ACM, Jouanin L, Kunert KJ, Rennenberg H, Foyer CH. Glutathione: biosynthesis, metabolism and relationship to stress tolerance explored in transformed plants. J. Exp. Bot. 1998; 49:623–647.

Ong ES, Zou L, Li S, Cheah PY, Eu KW, Ong CN. Metabolic profiling in colorectal cancer reveals signature metabolic shifts during tumorigenesis. Mol. Cell. Proteomics. 2010:M900551–MCP200.

Perera FP, Tang D, Wang S, Vishnevetsky J, Zhang B, Diaz D, Camann D, Rauh V. Prenatal polycyclic aromatic hydrocarbon (PAH) exposure and child behavior at age 6-7 years. Environ. Health Perspect. 2012; 120:921–926. [PubMed: 22440811]

Prosser GA, Larrouy-Maumus G, Carvalho LPS. Metabolomic strategies for the identification of new enzyme functions and metabolic pathways. EMBO Rep. 2014; 15:657–669. [PubMed: 24829223]

Razali NM, Wah YB. Power comparisons of shapiro-wilk, kolmogorov-smirnov, lilliefors and anderson-darling tests. J. Stat. Model. Analytics. 2011; 2:21–33.

Reimers MJ, La Du JK, Periera CB, Giovanini J, Tanguay RL. Ethanol-dependent toxicity in zebrafish is partially attenuated by antioxidants. Neurotoxicol. Teratol. 2006; 28:497–508. [PubMed: 16904866]

Ringuet J, Albinet A, Leoz-Garziandia E, Budzinski H, Villenave E. Diurnal/nocturnal concentrations and sources of particulate-bound PAHs, OPAHs and NPAHs at traffic and suburban sites in the region of Paris (France). Sci. Total Environ. 2012; 437:297–305. [PubMed: 22947617]

Roh T, Kwak MY, Kwak EH, Kim DH, Han EY, Bae JY, Lee BM. Chemopreventive mechanisms of methionine on inhibition of benzo(a)pyrene–DNA adducts formation in human hepatocellular carcinoma HepG2 cells. Toxicol. Lett. 2012; 208:232–238. [PubMed: 22138271]

Ruxton GD. The unequal variance t-test is an underused alternative to Student's t-test and the Mann–Whitney U test. Behav. Ecol. 2006; 17:688–90.

Sastre J, Pallardó FV, Viña J. Glutathione, oxidative stress and aging. Age. 1996; 19:129–139.

Santoro MM. Zebrafish as a model to explore cell metabolism. Trends Endocrinol. Metab. 2014; 25:546–554. [PubMed: 24997878]

Schioppa T, Uranchimeg B, Saccani A, Biswas SK, Doni A, Rapisarda A, Sica A. Regulation of the chemokine receptor CXCR4 by hypoxia. J. Exp. Med. 2003; 198:1391–1402. [PubMed: 14597738]

Seth A, Stemple DL, Barroso I. The emerging use of zebrafish to model metabolic disease. Dis. Model Mech. 2013; 6:1080–1088. [PubMed: 24046387]

Shen W, Yu Y. Translation initiation proteins, ubiquitin–proteasome system related proteins, and 14-3-3 proteins as response proteins in FL cells exposed to anti-benzo[a]pyrene-7, 8-dihydrodiol-9, 10-epoxide. Proteomics. 2008; 8:3450–3468. [PubMed: 18752215]

Shen G, Tao S, Wang W, Yang Y, Ding J, Xue M, Russell AG. Emission of oxygenated polycyclic aromatic hydrocarbons from indoor solid fuel combustion. Environ. Sci. Technol. 2011; 45:3459–3465. [PubMed: 21375317]

Shen H, Huang Y, Wang R, Zhu D, Li W, Shen G, Wang B, Zhang Y, Chen Y, Lu Y, Chen H, Li T, Sun K, Li B, Liu W, Liu J, Tao S. Global atmospheric emissions of polycyclic aromatic hydrocarbons from 1960 to 2008 and future predictions. Environ. Sci. Technol. 2013; 47:6415–6424. [PubMed: 23659377]

Skovlund E, Fenstad GU. Should we always choose a nonparametric test when comparing two apparently nonnormal distributions? J. Clin. Epidemiol. 2001; 54:86–92. [PubMed: 11165471]

Smith CA, O'Maille G, Want EJ, Qin C, Trauger SA, Brandon TR, Siuzdak G. METLIN: a metabolite mass spectral database. Ther. Drug Monit. 2005; 27:747–751. [PubMed: 16404815]

Suhre K, Gieger C. Genetic variation in metabolic phenotypes: study designs and applications. Nat. Rev. Genet. 2012; 13:759–769. [PubMed: 23032255]

Tang D, Li TY, Liu JJ, Zhou ZJ, Yuan T, Chen YH, Rauh VA, Xie J, Perera F. Effects of prenatal exposure to coal-burning pollutants on children's development in China. Environ. Health Perspect. 2008; 116:674–679. [PubMed: 18470301]

Timme-Laragy AR, Van Tiem LA, Linney EA, Di Giulio RT. Antioxidant responses and NRF2 in synergistic developmental toxicity of PAHs in zebrafish. Toxicol. Sci. 2009; 109:217–227. [PubMed: 19233942]

Van Tiem LA, Di Giulio RT. AHR2 knockdown prevents PAH-mediated cardiac toxicity and XRE- and ARE-associated gene induction in zebrafish (Danio rerio). Toxicol. Appl. Pharmacol. 2011; 254:280–287. [PubMed: 21600235]

Vignet C, Le Menach K, Lyphout L, Guionnet T, Frère L, Leguay D, Bégout ML. Chronic dietary exposure to pyrolytic and petrogenic mixtures of PAHs causes physiological disruption in zebrafish—part II: behavior. Environ. Sci. Pollut. Res. Int. 2014; 21:13818–13832. [PubMed: 24671398]

Vignet C, Devier MH, Le Menach K, Lyphout L, Potier J, Cachot, Cousin J. Long-term disruption of growth, reproduction, and behavior after embryonic exposure of zebrafish to PAH-spiked sediment. Environ. Sci. Pollut. Res. Int. 2014; 21:13877–13887. X. [PubMed: 24659400]

Welch BL. The significance of the difference between two means when the population variances are unequal. Biometrika. 1937; 29:350–62.

Weigand H, Totsche KU, Kogel-Knabner I, Annweiler E, Richnow HH, Michaelis W. Fate of anthracene in contaminated soil: transport and biochemical transformation under unsaturated flow conditions. Eur. J. Soil Sci. 2002; 53:71–81.

Wu J, Hou H, Ritz B, Chen Y. Exposure to polycyclic aromatic hydrocarbons and missed abortion in early pregnancy in a Chinese population. Sci. Total Environ. 2010; 408:2312–2318. [PubMed: 20219237]

Xia J, Psychogios N, Young N, Wishart DS. MetaboAnalyst: a web server for metabolomic data analysis and interpretation. Nucl. Acids Res. 2009; 37:W652–660. [PubMed: 19429898]

Xia J, Mandal R, Sinelnikov IV, Broadhurst D, Wishart DS. MetaboAnalyst 2.0—a comprehensive server for metabolomic data analysis. Nucleic Acids Res. 2012; 40:W127–W133. [PubMed: 22553367]

Xia T, Korge P, Weiss JN, Li N, Venkatesen MI, Sioutas C, Nel A. Quinones and aromatic chemical compounds in particulate matter induce mitochondrial dysfunction: implications for ultrafine particle toxicity. Environ. Health Perspect. 2004; 112:1347–1358. [PubMed: 15471724]

Xia Y, Cheng S, He J, Liu X, Tang Y, Yuan H, He L, Lu T, Tu B, Wang Y. Effects of subchronic exposure to benzo[a]pyrene (B[a]P) on learning and memory, and neurotransmitters in male Sprague-Dawley rat. Neurotoxicology. 2011; 32:188–198. [PubMed: 21216261]

Zhou B, Xiao JF, Tuli L, Ressom HW. LC-MS-based metabolomics. Mol. BioSyst. 2012; 8:470–481. [PubMed: 22041788]

Zhu ZJ, Schultz AW, Wang J, Johnson CH, Yannone SM, Patti GJ, Siuzdak G. Liquid chromatography quadrupole time-of-flight mass spectrometry characterization of metabolites guided by the METLIN database. Nat. Protoc. 2013; 8:451–460. [PubMed: 23391889]

Highlights

We used the zebrafish model to investigate differential polycyclic aromatic hydrocarbon (PAH) toxicity.

We investigate the metabolomic profiles produced by developmental PAH exposures.

We compared the metabolomic profiles produced by two environmentally abundant oxygenated PAHs.

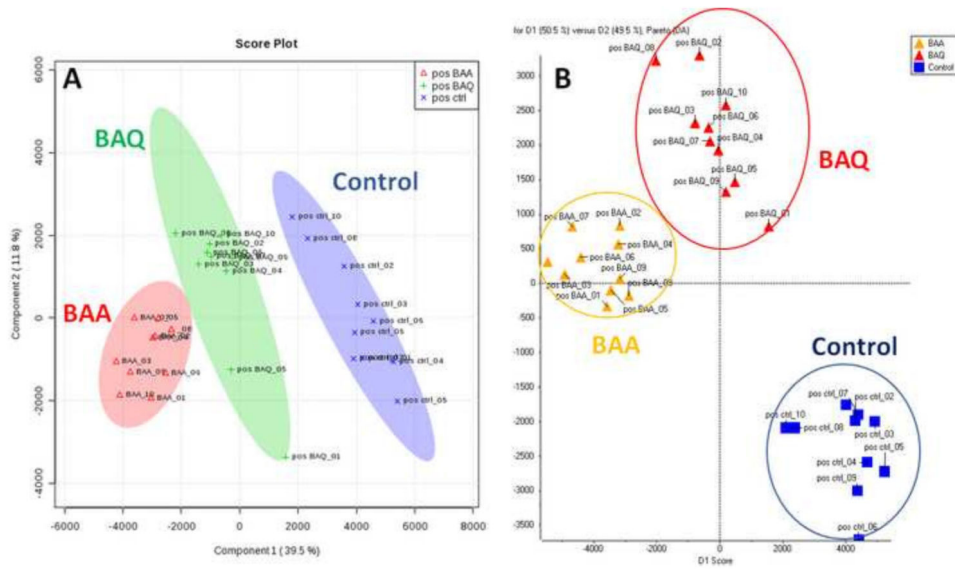Pathway analysis identified several perturbed molecular networks.

Figure 1.
PLS-DA score plot (A) and PCA-DA score plot (B) in the positive ion mode based on the normalized data.
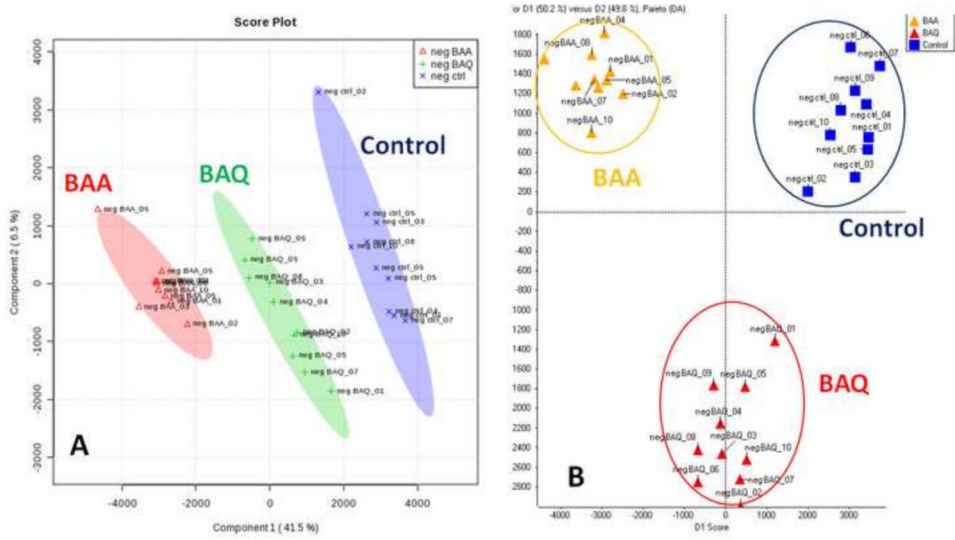
Figure 2.
PLS-DA score plot (A) and PCA-DA score plot (B) in negative ion mode based on the normalized data.
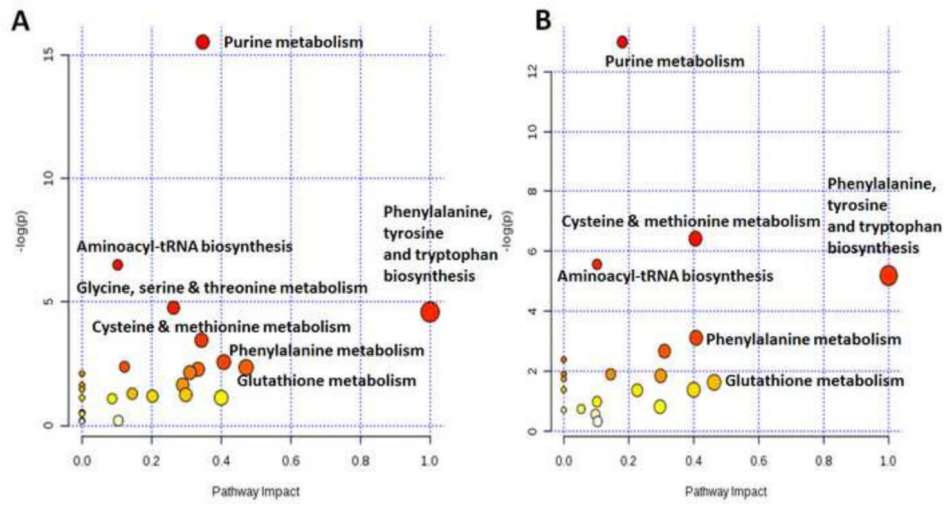
Figure 3.
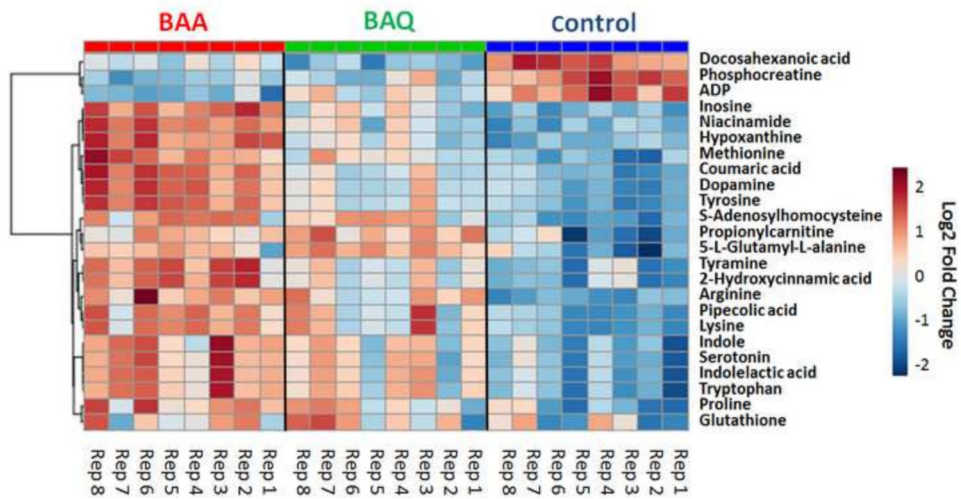Global metabolic disorders of the most relevant pathways influenced by (A) BAA and (B) BAQ treatment

Figure 4.
Heat map produced by hierarchical clustering of the most significantly different metabolites obtained from the positive ion mode. The log2 fold change in metabolite levels is color-coded: red pixels denote up regulation; blue pixels denote down regulation. Fold changes were based on peak intensities and relative to a pooled average sample from the control group.